

# PRECISE CAVITY TUNING SYSTEM OF A LOW OUTPUT-IMPEDANCE SECOND-HARMONIC CAVITY AT ISIS

Y. Irie<sup>#</sup>, S. Fukumoto, K. Muto, H. Nakanishi, KEK, Ibaraki, Japan  
 D. Allen, D. Bayley, N. Farthing, I. Gardner, R. Mathieson, A. Seville, J. Thomason  
 STFC/RAL/ISIS, Didcot, UK  
 J. Dooling, D. Horan, R. Kustom, M. Middendorf, ANL, Argonne, USA

## Abstract

A very low output-impedance ( $\sim 35$  ohms) second-harmonic cavity system is being developed for high intensity proton accelerators [1]. The final amplifier is comprised of a grounded cathode scheme with a feedback loop from anode to grid. Due to the Miller effect, the grid voltage waveform is seriously distorted even if only a few percent of sub-harmonic or higher harmonic are mixed in the driver current. Such distortion is much enhanced by the beam loading. In order to eliminate the effect of this distortion upon the phase detector used to achieve precise cavity tuning, a swept bandpass filter was applied to the grid voltage at the phase detector input. Filter design details and the result of high power tests are reported.

## INTRODUCTION

Beam loading compensation is essential for the low loss operation of high intensity accelerators. Beam feedforward technique is widely used for this purpose [2,3]. Low output-impedance configuration of the tube, such as cathode follower, however, has only been used as a beam buncher in a proton storage ring [4]. Since the voltage gain of the cathode follower is less than unity and the power efficiency is not high, a power saving scheme with high voltage gain has been investigated [5]. In the new scheme, which is called LOI (Low Output-Impedance) hereafter, the final triode amplifier comprises a grounded cathode scheme with a feedback loop from anode to grid. The voltage gain is then higher than 20 over a frequency range 2 ~ 6 MHz, and the output impedance ( $Z_{out}$ ) is  $\sim 30$  ohms [1, 6]. However, due to the Miller effect of the final amplifier, the grid voltage waveform is seriously distorted by only a few percent content of sub-harmonic or higher harmonic in the driver current [1]. Such distortions made it difficult to precisely compare the phases of grid and cavity voltages for ferrite cavity tuning. The sub-harmonic originates in the master oscillator, and the higher harmonic is thought to be generated by the non-linear response of the driver amplifier. Initially, we examined elimination of the sub-harmonic content in the master oscillator. However, since such distortion is much enhanced by the beam loading, elimination only in the

master oscillator is not sufficient. We then decided to apply a bandpass filter at the input of the phase detector. The frequency region of the bandpass filter is swept at 50 Hz. By using the filter, the bias tuning loop of the second-harmonic cavity was stabilized. In this report, filter design detail, results of high power tests and an alternative detection method using grid input current or cavity input current, are described. Finally, comparison of feedforward and low-impedance schemes is briefly discussed from the view point of parameter drift/variation of the final amplifier.

## SWEPT BANDPASS FILTER

The frequency sweep of LOI and the neighbouring harmonics are shown in Fig. 1. In order to eliminate these harmonics, the passband should be divided into 3 parts at least:

$$\begin{aligned} \text{Passband} \\ &= [2.60, 3.90] \text{ MHz} && \text{for } 0 < t < 4.1 \text{ ms,} \\ &= [3.90, 5.85] \text{ MHz} && \text{for } 4.1 < t < 8.0 \text{ ms, (1)} \\ &= [5.85, 6.20] \text{ MHz} && \text{for } 8.1 < t < 10 \text{ ms.} \end{aligned}$$

The swept bandpass filter (SBPF) was designed for this purpose using the NI FlexRIO FPGA Module (PXIe-7962R). The clock frequency is 100 MHz, and the time delay is 1.87  $\mu$ s. Actually, the passband comprises 6 units rather than 3 in Eq. (1) so that each unit has a narrower bandwidth. Fig. 2 shows FFT spectra of the grid voltage at 9.5 ms for the cases with and without the SBPF.

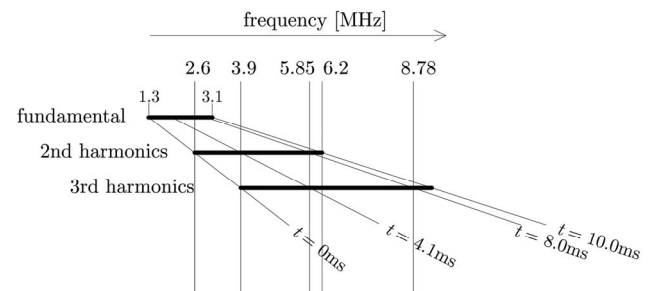


Figure 1: Variation of harmonic frequency with time during the acceleration phase. Frequency range of LOI is given at the middle line, 2.6 ~ 6.2 MHz.

The gap voltage shows a purely sinusoidal waveform due to the high Q cavity. However, in order to compensate for the time delay of the grid voltage in the

SBPF, the delay equalizer of 1.87  $\mu$ s is implemented at the gap voltage input of the phase detector (Fig. 3). The phase detector output is fed back to the cavity bias current supply for tuning.

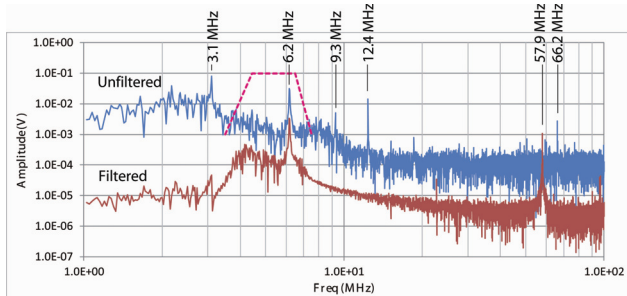


Figure 2: Response of swept bandpass filter upon grid voltage at 9.5 ms, when the LOI frequency is 6.2 MHz. Dashed line shows SBPF bandwidth.

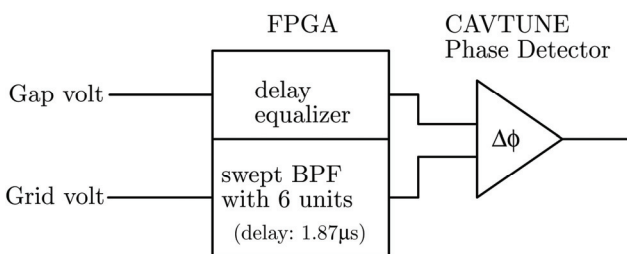


Figure 3: Swept bandpass filter and equalizer functions are realized by the FPGA module.

### EXPERIMENTAL RESULTS

Fig. 4 compares the grid voltage waveforms before and after the SBPF. The 2nd harmonic component is well shaped by the SBPF, although 60 MHz component can still be seen after the filter at 9.5 ms (see Fig. 2): reason is to be investigated. The phase detector output was also improved by more than a factor of four as shown in Fig. 5. The bias tuning loop was then stabilized and generation of high gap voltage at 10 kV-peak became possible

### OPTIMIZATION OF PHASE DETECTION METHOD

Other potential candidates for phase detector input signal are the cavity input current and the grid input current.

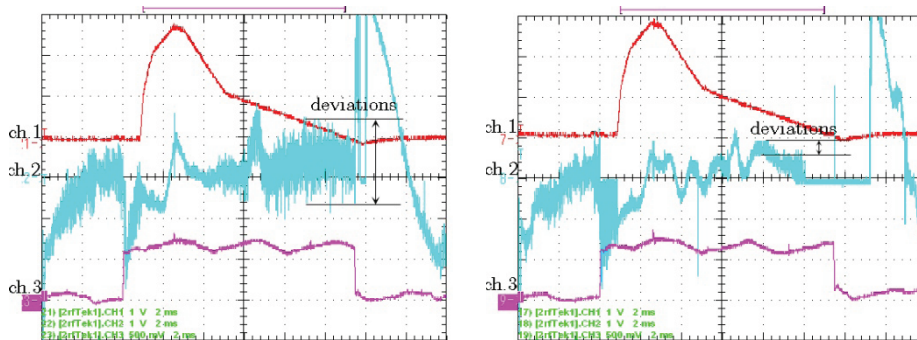


Figure 5: Comparison of phase detector output between unfiltered (left) and filtered (right) cases. Ch1: gap volts envelope (1V=1.2 kV-peak), Ch2: phase detector output (1V=10 deg.), and Ch3: anode supply current (30A/V).

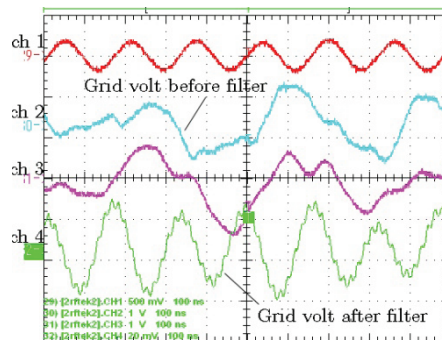


Figure 4: Waveforms at 9.5 ms. Even after the filter, ~60MHz spikes can be seen in the grid volt waveforms. Ch1: gap volt, Ch2: grid volt filter input, Ch3: cavity input current, Ch4: grid volt monitor (filtered).

The tuning sensitivities for these signals and the grid voltages were compared using SPICE simulations. Tuning sensitivity, having the units of degree/MHz, is defined as the derivative phase difference from the gap voltage at resonance. Two resonant modes were considered. One is that only the cavity is at resonance, and the other that the final triode current is at the minimum. The latter case implies whole load connecting to the triode anode is at resonance, including the anode choke and any stray capacitances across the triode.

Fig. 6 shows the simulation results. In the minimum triode current mode, cavity input current has high sensitivity at early stages, but loses it rapidly towards the middle. In contrast, grid voltage starts with a lower value, and increases gradually toward the end. Grid current always has the lowest sensitivity as expected, because the driver amplifier, which has a high output impedance (~5 k $\Omega$ ), almost acts as a constant current generator and is insensitive to any change of impedance looking into the final triode. In the cavity resonant mode, the cavity input current shows very high and constant sensitivity over the whole cycle. The constancy comes from the fact that the cavity shunt impedance was assumed to be constant (538  $\Omega$  [7]). The phase shift ( $\Delta\phi$ ) due to frequency change at the cavity resonance is given by

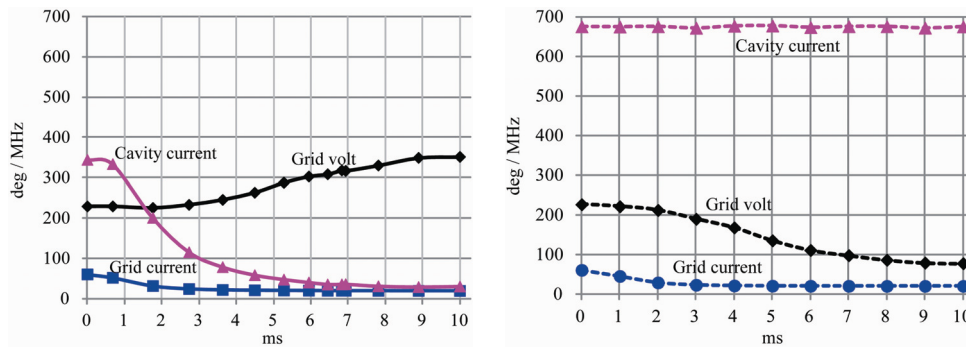


Figure 6: Sensitivity analysis in minimum triode current mode (left) and cavity resonant mode (right).

$$\tan(\Delta\phi) = 2Q \frac{\Delta\omega}{\omega_0}$$

$$\therefore \frac{\Delta\phi}{\Delta\omega} \cong 2RC = 682 \text{ deg / MHz}, \quad \Delta\phi \ll 1.$$

Here  $R$  is the cavity shunt impedance and  $C$  the total gap capacitance, 1,760 pF.

Although the cavity input current has such a superior characteristic in the cavity resonant mode, this scheme is not appropriate because the maximum available power of the triode is limited. Grid voltage is a better signal from the view point of overall sensitivity and power efficiency. The phase difference between grid and gap voltages at resonance is 182 deg. at the beginning of acceleration, and tends to 205 deg. at the end. These differences can be realized by changing a delay time in the delay equalizer in Fig. 3.

### COMPARISON OF BEAM FEEDFORWARD AND LOI Schemes

It is obvious that both the beam feedforward and LOI can reduce the output impedance to 1/30~1/40 of the original cavity impedance. However, it is interesting to compare the two methods from view point of gain change due to long-term drift and/or shift of the operating point of the final amplifier.

Fig. 7 shows how the impedance reduction is realized by the beam feedforward. In the figure impedance reduction rate of 1/30 is assumed. However, if the final amplifier gain is decreased by 5 %, the output impedance will be increased by 145 %, resulting in a reduction rate of 1/12. Re-adjustment of feedforward gain or replacement of the tube will be required. In the LOI, output impedance is given by,

$$Z_{\text{out}} \cong \frac{r_p}{1 + \mu\beta}$$

$$\cong r_p / \mu\beta,$$

where  $r_p$  is the plate resistance,  $\mu$  the amplification factor of the final amplifier and  $\beta$  the voltage feedback ratio. Since  $Z_{\text{out}}$  depends linearly upon  $\mu$ , 5 % decrease of  $\mu$  yields an increase of  $Z_{\text{out}}$  by the same amount. It is

therefore clear that the LOI is less vulnerable to the parameter changes of the final amplifier.

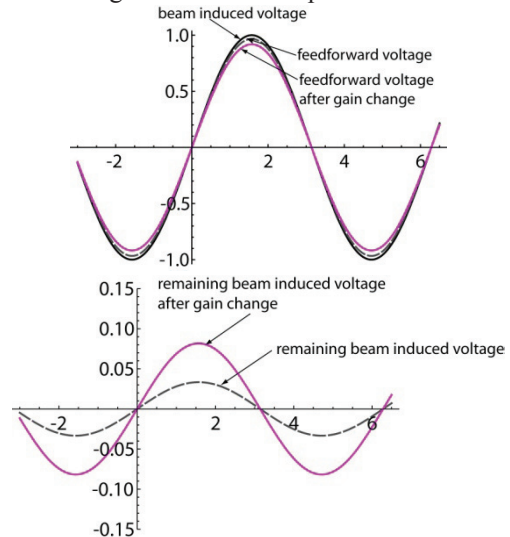


Figure 7 : Beam induced voltage and its compensation (upper), and remaining induced voltage after subtraction of compensation (lower) which is proportional to reduced output impedance.

### REFERENCES

- [1] Y. Irie et al., "First Beam Experiments at ISIS with a Low Output-impedance Second Harmonic Cavity," IPAC2011, San Sebastian, WEPS025, p. 2538 (2011); <http://www.JACoW.org>
- [2] IP. Barratt et al., "RF System and Beam Loading Compensation on the ISIS Synchrotron," EPAC90, Nice, p.949 (1990); <http://www.JACoW.org>
- [3] F. Tamura et al., Phys. Rev. ST Accel. Beams 14, 051004 (2011).
- [4] T. Hardek, "A Low-impedance, 2.8-MHz, Pulsed Bunching System for the Los Alamos Proton Storage Ring," LA-UR-84-1935: submitted to 16<sup>th</sup> Power Modulator Symposium, Arlington, 1984.
- [5] <http://research.kek.jp/group/www-loi/>
- [6] T. Oki et al., Nucl. Instrum. and Methods in Phys. Res. A 565 (2006) pp. 358-369.
- [7] LOI progress report LOI-2, 2005, available at [5].